

# Hybrid simulation of ion cyclotron resonance in the solar wind: Evolution of velocity distribution functions

Xing Li

Institute of Mathematical and Physical Sciences, University of Wales, Aberystwyth, UK

Shadia R. Habbal

Institute for Astronomy, University of Hawaii, Hawaii, USA

Received 25 January 2005; revised 17 July 2005; accepted 25 July 2005; published 29 October 2005.

[1] Resonant interaction between ions (oxygen ions  $O^{+5}$  and protons) and ion cyclotron waves is investigated using a one dimensional hybrid code. Ion cyclotron waves are self-consistently generated by an ion cyclotron anisotropy instability. We focus on the detailed acceleration process of ions. The energization of oxygen ions due to waves is found to have two stages. During the first stage, oxygen ions are energized by ion cyclotron waves in the direction perpendicular to the background magnetic field and can develop extreme high temperature anisotropies with  $T_{O\perp}/T_{O\parallel} \approx 22$  in an initially low beta plasma (beta value at 0.01) with very little parallel heating. During this stage, oxygen ions do not show an appreciable bulk acceleration along the background magnetic field. In the second stage, a large bulk acceleration of oxygen ions as large as  $0.3v_A$ , where  $v_A$  is the Alfvén speed, is observed. Ion cyclotron waves are not able to maintain a high temperature anisotropy as inferred from observations. The nonlinear nature of wave particle interaction produces highly complex velocity distribution functions in the oxygen ions. In contrast, the heating and acceleration behavior of the major species, namely protons, is quite different. The velocity distribution functions of protons are less complex than the oxygen velocity distributions. Protons can also develop a large temperature anisotropy with preferential heating in the perpendicular direction. A bulk acceleration of protons (much smaller than the acceleration of oxygen ions) along the background magnetic field is observed to develop simultaneously with the development of a proton temperature anisotropy.

**Citation:** Li, X., and S. R. Habbal (2005), Hybrid simulation of ion cyclotron resonance in the solar wind: Evolution of velocity distribution functions, *J. Geophys. Res.*, *110*, A10109, doi:10.1029/2005JA011030.

## 1. Introduction

[2] Observations from the Ultraviolet Coronagraph Spectrometer (UVCS) and Solar Ultraviolet Measurements of Emitted Radiation (SUMER) on board the Solar and Heliospheric Observatory (SOHO) have significantly enhanced our understanding of the coronal heating and solar wind acceleration. In the solar wind primary acceleration region, i.e., the first few solar radii, oxygen ions have been carefully observed. UVCS observations reveal that the oxygen  $O^{+5}$  ions not only have greater than mass-proportional temperatures in the inner corona, they are also much faster than protons and have much higher perpendicular (to the magnetic field) than parallel temperatures as well [Kohl *et al.*, 1998; Li *et al.*, 1998; Cranmer *et al.*, 1999]. SUMER spectral line observations at the base of the corona in a southern coronal hole indicate that the temperature of minor

ions decreases with increasing mass per charge [Tu *et al.*, 1998]. These studies strongly indicate that ion cyclotron resonance may play an important role in coronal heating. Consequently, over the past few years, particular attention has been paid to parallel propagating ion cyclotron waves as a mechanism for the coronal heating and solar wind acceleration. These include fluid models [Cranmer *et al.*, 1999, 2000; Hollweg, 1999, 2000; Hu and Habbal, 1999; Li *et al.*, 1999; Li and Habbal, 1999; Li, 2003; Tu and Marsch, 2001] and kinetic (or semi-kinetic) models [Galinsky and Shevchenko, 2000; Isenberg, 2004; Isenberg *et al.*, 2001; Liewer *et al.*, 2001; Tam and Chang, 2001; Vocks and Marsch, 2001, 2002; Vocks, 2002]. Hollweg and Isenberg [2002] gave a thorough review on this topic. Fluid models assume that ions have Maxwellian or bi-Maxwellian velocity distributions. The interaction between waves and particles is accounted for by adopting a quasi-linear theory [Arunasalam, 1976; Dusenbery and Hollweg, 1981; Marsch *et al.*, 1982]. Kinetic models allow the departure of particle velocity distributions from Maxwellian or bi-Maxwellian.

However, kinetic models also introduce complications, e.g. the treatment of wave dispersion. Indeed, the exact nature of ion cyclotron waves in a plasma with complex velocity distributions is not analytically known. However, the adoption of quasi-linear theory requires knowledge of the property of these waves.

[3] The evolution of ion velocity distributions under the influence of ion cyclotron waves is important for our understanding of coronal heating and solar wind acceleration problem. This issue has already attracted some attention. Using hybrid codes, *Ofman et al.* [2001] and *Gary et al.* [2001] found that the high temperature anisotropy reported by *Cranmer et al.* [1999] will decline rapidly owing to ion cyclotron instabilities. Hence they concluded that the observed high temperature anisotropy can only be maintained when some mechanisms, presumably ion cyclotron waves, which produce the anisotropy, are continuously at work. Again using a hybrid code, *Ofman et al.* [2002] investigated the heating of protons and oxygen ions by introducing a broadband spectrum of ion cyclotron waves. They found oxygen ions can have complex velocity distributions under the influence of ion cyclotron waves while protons may still have roughly bi-Maxwellian distribution functions. Perhaps owing to the weak wave amplitudes adopted, the acceleration of oxygen ions is quite weak in their studies. Detailed evolution of particle velocity distribution functions were not given. More recently, *Xie et al.* [2004] also studied the resonant interaction between solar wind ions and ion cyclotron waves using a hybrid simulation. They try to explain how the driving spectrum frequency range and the power law index affect the resonant heating, and the effect of differential flows on the resonant interaction. A more realistic application of ion cyclotron waves in the solar wind was modeled in an expansion box model using a flat wave spectrum [*Liewer et al.*, 2001]. In this model, ion cyclotron resonance was studied after the solar wind acceleration is already completed. They found in both high and low plasma beta cases that the preferential acceleration and heating of heavy ions (alpha particles) are limited. Recently, *Lu and Wang* [2005] also studied ion cyclotron resonance using hybrid simulations. They found preferential heating of protons and alpha particles in the direction perpendicular to the background magnetic field. However, the acceleration of the alpha particles is quite small.

[4] We tackle the evolution of ion velocity distributions under the influence of ion cyclotron waves with a different approach. A third ion species  $\text{Li}^{+1}$  with initial bi-Maxwellian velocity distributions is introduced into the system. These  $\text{Li}^{+1}$  ions are unstable to ion cyclotron waves and the generated waves will then be used to heat protons and oxygen ions. The scenario may simulate the case where ion cyclotron waves in the solar wind are generated locally [*Cranmer*, 2000]. The advantage of this approach is that ion cyclotron waves are introduced fully self-consistently. If a spectrum of ion cyclotron waves is introduced as in the work by *Ofman et al.* [2002], it is quite difficult to self-consistently (by considering wave dispersion relations) introduce electric field components of the waves and perturbations of velocity distributions (this is especially the case if the wave amplitude is strong; hence waves are nonlinear). Possible effects of wave nonlinearity have to be neglected. The disadvantage of our approach is that we need

to take far more particles to reduce high frequency noise. Because instabilities need a certain time to develop, our approach is also more demanding in computer time and we are only able to explore the effect of ion cyclotron waves on ions with a relatively large amplitude. Another difference we have to bear in mind is that externally driven waves propagate primarily away from the Sun so that low-frequency resonances are primarily with ions moving toward the Sun, while instability-driven waves may resonate with both sunward and anti-sunward moving ions.

## 2. Simulation Code

[5] A one-dimensional electromagnetic hybrid simulation code is adopted to conduct this work [*Winske and Omid*, 1993]. Various ions species are treated kinetically via standard particle-in-cell methods used in particle codes and the electrons are treated as a single charge neutralizing massless fluid. We consider a collisionless, magnetized, homogeneous plasma. The background magnetic field  $B_0$  is along the  $x$  direction. About 1.5 million particles of each species are uniformly distributed over 128 cells and the length of each cell is  $c/\omega_p$ . Here  $\omega_p$  is the proton plasma frequency. The integration time step is  $\Omega_p \Delta t = 0.02$ . The number of particles used will in general affect the fluctuation level of high frequency noise but does not influence the overall results of the investigation. However, it is found that more particles will delay the onset of the ion cyclotron instability.

[6] We study ion cyclotron resonant heating in a low beta Vlasov plasma. The plasma ions consist of protons, lithium ions, and oxygen ions  $\text{O}^{+5}$ . To introduce low-frequency ion cyclotron waves in the system, a third component  $\text{Li}^{+1}$  is introduced in the system. Initially the  $\text{Li}^{+1}$  has bi-Maxwellian velocity distributions and is highly anisotropic ( $T_{\perp}/T_{\parallel} = 9$ ). So this component is used to launch ion cyclotron waves with frequency less than the proton gyrofrequency. Note a temperature anisotropy instability can launch waves in both parallel and anti-parallel directions. To simulate ion cyclotron resonance between coronal ions and parallel propagating ion cyclotron waves originating from the Sun, the  $\text{Li}^{+1}$  is given a drift flow of one Alfvén speed defined as  $v_A = B_0/\sqrt{4\pi n_e m_p}$ . The background magnetic field  $B_0$  is along the  $x$ -direction. The plasma beta value of species  $j$  is defined as  $\beta_j = 8\pi n_e k_B T_{\parallel j}/B_0^2$ , the  $j$ th species thermal speed  $U_j = \sqrt{2k_B T_{\parallel j}/m_j}$ , and the gyrofrequency,  $\Omega_j = e_j B_0/m_j c$ . The initial condition is:  $\beta_e = \beta_p = 0.01$ ,  $\beta_{\text{Li}} = 1$ , protons are isotropic;  $n_{\text{Li}}/n_e = 0.075$ .

[7] Linear Vlasov theory predicts that the instability will launch waves propagating in both the direction of the drifting  $\text{Li}^{+1}$  and the direction opposite to this drift. The detailed dispersion relation for these two instabilities is shown in Figure 1. The code to calculate the dispersion relation in Figure 1 is the same as the one used by *Li and Habbal* [1999]. Note that owing to Doppler effect, waves propagating in the direction opposite to the drifting ions have much smaller frequencies than the parallel propagating waves. To show the resonance properties of ions with parallel and anti-parallel propagating fluctuations, the real part of the cyclotron resonance factor

$$\xi_j^{\pm} = \frac{\omega - k \cdot v \pm \Omega_j}{kU_j} \quad (1)$$

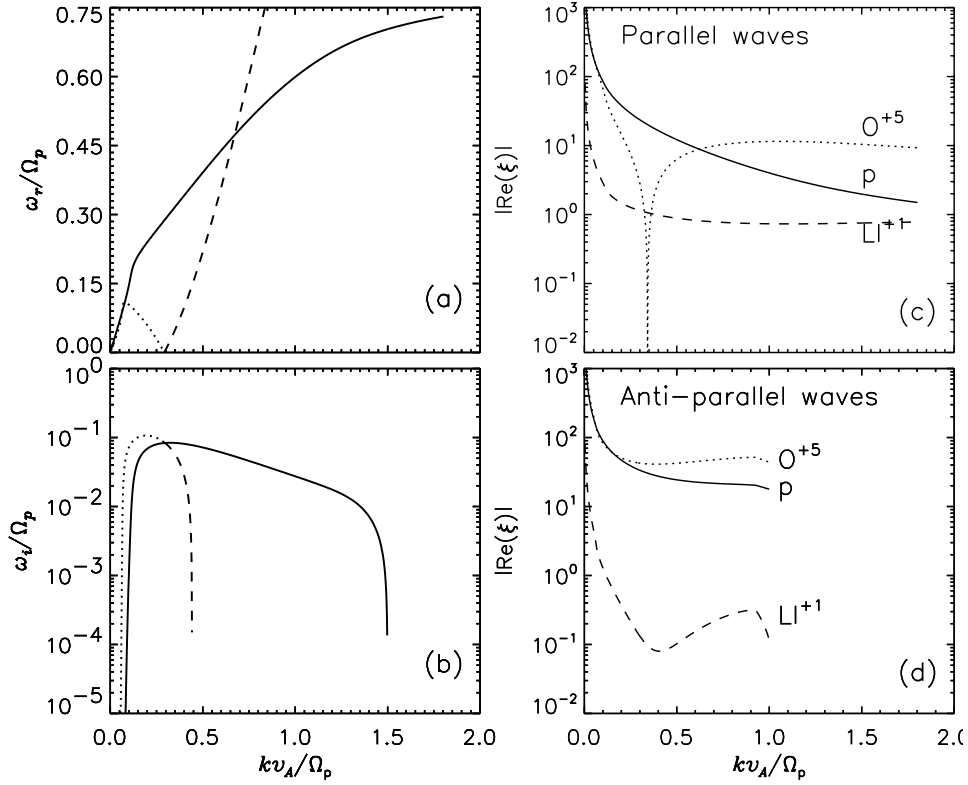


**Figure 1.** (a) Dispersion relation of parallel (solid line) and anti-parallel (dotted line) propagating ion cyclotron waves excited by drifting anisotropic  $\text{Li}^{+1}$  with drifting velocity  $1v_A$ . The dashed line represents right-hand polarized parallel propagating waves. In the frame of drifting  $\text{Li}^{+1}$ , these waves are anti-parallel ion cyclotron waves. (b) Their corresponding growth rates. The absolute value of the real of resonance factors for (c) parallel propagating ion cyclotron waves and (d) anti-parallel propagating waves.

for different ions is shown in (Figure 1c (1d)) for parallel (anti-parallel) waves. Here  $v$  is the average flow speed of species  $j$  along the background magnetic field and  $k$  is the parallel wave number. In Figure 1c, sign “+” is taken. In Figure 1d, the plus sign is also used. However, when  $kv_A/\Omega_p > 0.6$ , the minus sign is used in the above equation for lithium ions (lithium ions resonate with these anti-parallel propagating waves in the rest frame of lithium). If  $|\text{Re}(\xi_j^\pm)|$  is much greater than 1, ions  $j$  do not resonate with waves. If  $|\text{Re}(\xi_j^\pm)|$  is much smaller than 1, then ions  $j$  strongly resonate with waves. If the resonance factor is about 1, a very weak resonance is expected.

[8] Figure 1 tells us that protons only weakly resonate with parallel propagating waves at high frequencies. Oxygen ions only strongly resonate with parallel propagating waves at their cyclotron frequency. Waves propagating in the direction opposite to the drifting ions (anti-parallel) are not in resonance with oxygen ions: the frequency in the unstable region is much smaller than oxygen gyrofrequency, apparently owing to the Doppler effect. This is clearly shown in Figure 1d, the oxygen resonance factor is much greater than 1 indicating no resonance. Lithium ions resonate with both parallel propagating and anti-propagating waves. The highest growth rate of these antiparallel waves is only slightly larger than the highest growth rate of parallel waves. Hence these antiparallel waves can contribute substantially to the total magnetic fluctuations. Note that

oblique waves can be launched as well, but these waves do not show up in our 1D simulation.

### 3. Results

[9] The temporal evolution of the averaged magnetic field component squared due to ion cyclotron instability is shown in Figure 2. Ion cyclotron anisotropy instability goes through a linear phase when  $0 \leq \Omega_p t \leq 100$  and wave amplitude increases exponentially until  $\Omega_p t \sim 100$ . Hereafter the instability is saturated. However, when  $\Omega_p t$  is between 100 and 200, the wave magnetic field has a local minimum. This local minimum is partly due to the resonant interaction between ion cyclotron waves and oxygen and protons (see Figures 4 and 5 in section 3.1). However, the local minimum is governed by the nonlinear behavior of the ion cyclotron anisotropy instability of the streaming Li ions. The temporal evolution of the parallel and perpendicular temperature, temperature anisotropy and flow speed of  $\text{Li}^{+1}$  ions is shown in Figure 3. Figure 3c demonstrates that in the linear stage of the ion cyclotron anisotropy instability ( $0 \leq \Omega_p t \leq 100$ ), the flow speed of  $\text{Li}^{+1}$  ions does not show a noticeable change. When the instability of  $\text{Li}^{+1}$  temperature anisotropy saturates ( $\Omega_p t \geq 250$ ), the temperature and its anisotropy as well as the flow speed of  $\text{Li}^{+1}$  change very little. Figure 3b shows that the temperature anisotropy of  $\text{Li}^{+1}$  ions does not decrease monotonically with time.

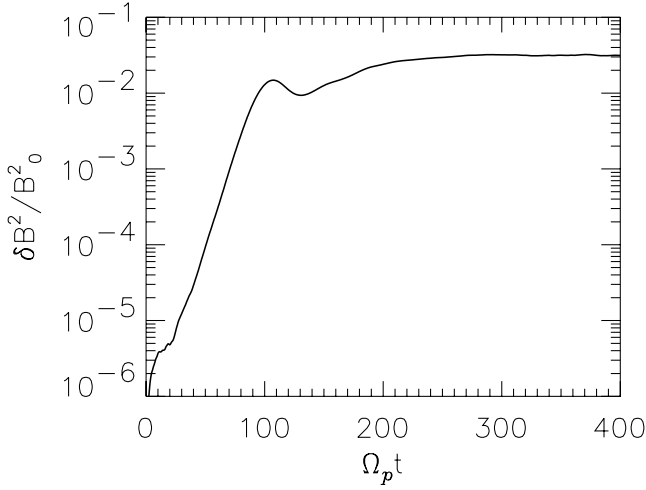


**Figure 2.** Temporal evolution of magnetic fluctuations  $\delta B^2/B_0^2$ .

Around  $\Omega_p t = 130$ , the temperature anisotropy  $T_{Li\perp}/T_{Li\parallel}$  actually increases slightly (Figure 3b). This can also be seen in the temperature profiles (Figure 3a). This suggests that ion cyclotron waves generated by  $\text{Li}^{+1}$  anisotropy instability heat Li ions substantially during this time period. The exact physical nature of this phenomenon is not known at this time. However, since the evolution of this temperature anisotropy instability is not the main subject of this paper, we will turn our attention to the evolution of oxygen ions and protons. (Note that the electromagnetic anisotropy instability driven by a heavy ion species with temperature anisotropy and initial flow speed relative to the protons has been studied by *Gary et al.* [2003]).

### 3.1. Heating of Oxygen Ions $\text{O}^{+5}$

[10] We now first describe the energization behavior of oxygen ions  $\text{O}^{+5}$ . The temporal evolution of  $\text{O}^{+5}$  is shown in Figure 4. Figure 4a demonstrates that  $\text{O}^{+5}$  ions are heated enormously. In hybrid simulations, temperatures are calculated by averaging over all particles. It is inevitable that the calculated temperatures will include the contributions from small wavelength waves excited in the system. Hence we may regard the calculated temperatures as kinetic temperatures. However, contributions from bulk flow speed in both parallel and perpendicular directions are excluded in the calculated kinetic temperatures. (Fluid velocity or bulk fluid velocity in a given direction is defined as the average velocity of all the particles in the simulation domain in that direction).

[11] The energization process of  $\text{O}^{+5}$  ions due to ion cyclotron resonance occurs in two stages. In the first stage ( $0 \leq \Omega_p t \leq 140$ ), the temperature anisotropy  $T_{O\perp}/T_{O\parallel}$  of  $\text{O}^{+5}$  increases rapidly and peaks at about 22. This peak value of oxygen anisotropy falls in the range reported by UVCS [*Cranmer et al.*, 1999]. During this stage,  $T_{O\perp}$  increases more than 40 times of its initial value but the parallel temperature  $T_{O\parallel}$  only increases by a factor of 2. Interestingly, during this stage, there is very little bulk acceleration along the background magnetic field. We may regard this stage as the linear stage of the cyclotron resonance between oxygen ions and ion cyclotron waves. After  $T_{O\perp}/T_{O\parallel}$  peaks at  $\Omega_p t \sim 140$ , the second stage of

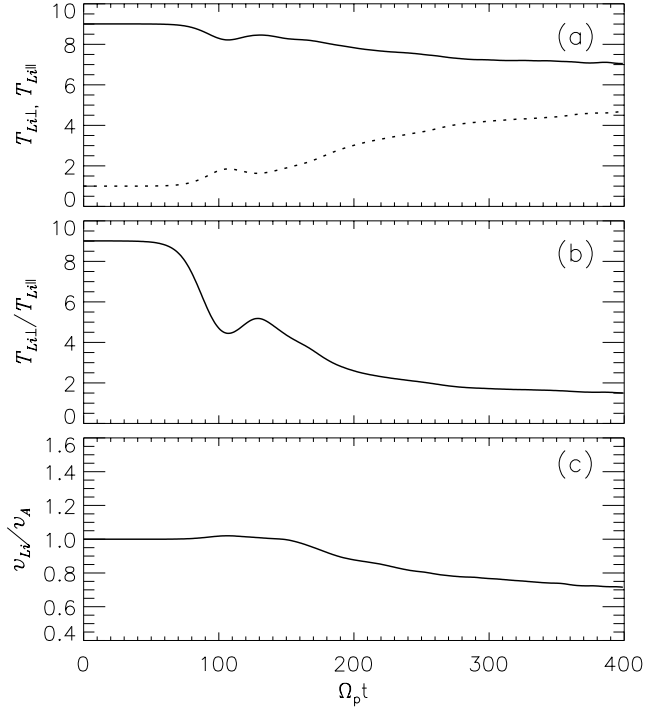


**Figure 3.** Evolution of (a)  $\text{Li}^{+1}$  parallel (dotted line) and perpendicular (solid line) temperature in units of the initial temperature, (b) temperature anisotropy  $T_{Li\perp}/T_{Li\parallel}$ , and (c) flow speed.

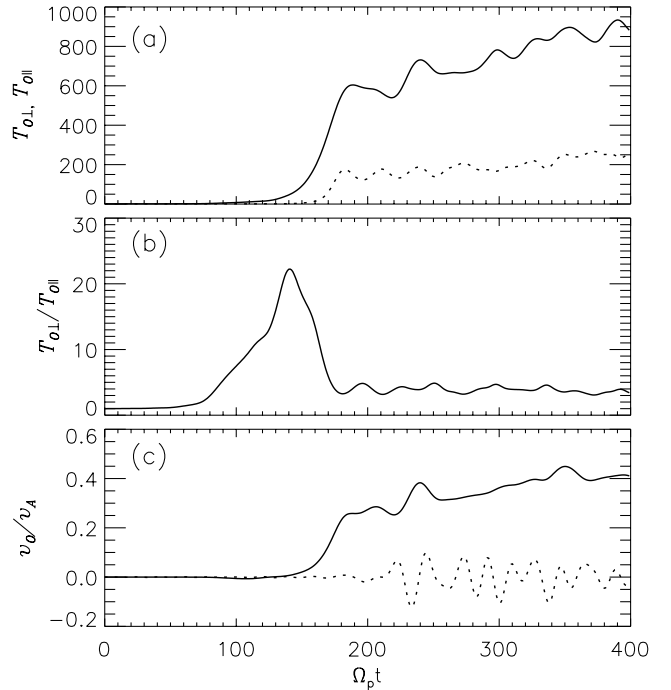


**Figure 4.** Evolution of (a)  $\text{O}^{+5}$  parallel (dotted line) and perpendicular (solid line) temperature, (b) temperature anisotropy  $T_{O\perp}/T_{O\parallel}$  (dotted line), and (c) flow speed along background magnetic field (solid line) and perpendicular fluid speed  $v_{\perp}$ . The temperatures are in units of the initial temperature.

oxygen energization begins. Indeed, a more dramatic heating and acceleration of oxygen ions occurs during this stage. Because the abundance of oxygen ions is very small ( $10^{-5}$ ), the resonant heating of oxygen ions  $O^{+5}$  removes little energy from ion cyclotron waves produced by  $Li^{+1}$  ions. As a result, oxygen ions are heated to extreme temperatures. Figure 4c shows the bulk acceleration of oxygen ions (solid line) that takes place during this stage. Compared with the study of *Ofman et al.* [2002], the acceleration of oxygen ions in our study is about 100 times stronger. Also plotted in Figure 4c is the y component of the perpendicular fluid velocity of oxygen ions  $v_y$  (dotted line) calculated by numerically integrating the moments of the oxygen velocity distributions. In the nonlinear stage of the resonant heating, this fluid velocity is significant (the amplitude can reach  $0.1v_A$ ), but is still much smaller than the thermal speed of oxygen ions. In Figure 4a, when the perpendicular temperature of oxygen ions reaches 800 times of its initial value, the thermal speed can be  $0.7v_A$ . The significant perpendicular fluid velocity can be easily understood since the waves generated in the system are at the gyrofrequency of oxygen ions. If we use symbols  $v_j^- = v_y - iv_z$  and  $E^- = E_y - iE_z$ , the fluid velocity of species  $j$  can be written as [Stix, 1992]

$$v_j^- = \frac{ie_j}{m_j} \frac{E^-}{\omega - \Omega_j},$$

in the cold plasma ( $T = 0$ ) approximation. Here  $E_y$  and  $E_z$  are the electric field components,  $v_y$  and  $v_z$  are the two fluid velocity components. Although this equation predicts that  $v_O^-$  will reach infinity at the oxygen gyrofrequency  $\omega = \Omega_O$ , thermal effects will limit this effect. For the major species protons, since  $\omega$  is always smaller than the proton gyrofrequency, the perpendicular fluid velocity of protons is expected to be small. We will see this in Figure 7 in section 3.2.

[12] Figure 4 also demonstrates that the temperature anisotropy of oxygen ions  $O^{+5}$  cannot maintain its peak value. One possible reason for this phenomenon is that the high temperature anisotropy of oxygen ions develops their own cyclotron instability [Ofman et al., 2001]. Under the sole influence of the temperature anisotropy instability of oxygen,  $T_{O\perp}$  will decrease, which is not observed in our simulations. Here the main reason for the anisotropy reduction is the parallel heating of oxygen ions by the cyclotron waves.

[13] To understand the oxygen energization process better, scatterplots of oxygen ions in the plane parallel and perpendicular to the background magnetic field at various times are shown in Figures 5 and 6, respectively. The two stage heating processes of oxygen ions can be seen clearly in Figure 5. Scatterplots in Figure 5 at  $\Omega_p t = 100, 120$  and  $140$  show that the oxygen ions have bi-Maxwellian-like velocity distributions at the early stage of cyclotron resonant heating (note the different scale in these plots) with  $T_\perp \gg T_\parallel$ . The overall scatterplots do not show appreciable shift in the parallel direction. However, scatterplots at  $\Omega_p t = 160, 168, 174$  and  $194$  have highly complicated structures. When oxygen ions are resonantly accelerated, they move forward in “beams” in phase space, leading to a bulk shift of the overall velocity distribution. It is interesting to note that

these scatterplots have some overall “shell like” shape if we ignore the detailed complex structure. The shell-like sense is more pronounced at  $\Omega_p t = 400$ . These “beams” are also unstable, they can rapidly evolve and the velocity distributions are randomized at  $\Omega_p t = 400$  when the simulation ends.

[14] Figure 6 shows the scatterplots of oxygen ions in the velocity plane perpendicular to  $v_\parallel$ . The oxygen beams shown in Figure 5 here appear as ring like structures. Note that at  $\Omega_p t = 168, 174$  and  $194$ , at the center of the scatter plots, there is a velocity void and the oxygen phase space looks like a ring. However, these structures are unstable and the scatterplots eventually randomize. At  $\Omega_p t = 400$  the scatter plot is nicely gyrotropic: it is close to a Maxwellian in the direction perpendicular to the background magnetic field. Figure 6 also shows that the center of the velocity distributions fluctuates at different times, indicating perpendicular fluid velocity fluctuations.

[15] In a plasma with a background magnetic field, positive ions gyrate around the magnetic field in a left hand sense. When a left-handed ion cyclotron wave is propagating parallel to the magnetic field, the electric field also gyrates around the magnetic field in a left-handed sense. A gyrating ion will find the wave electric field constant when the ion gyration or cyclotron frequency matches the wave frequency (the resonance condition). Hence ions can be constantly accelerated in the direction perpendicular to the magnetic field and a resonance occurs. Randomly distributed ions in velocity space accelerated in the direction perpendicular to the magnetic field lead to preferential heating of ions in the perpendicular direction.

[16] To understand the ring phase space structure, we need to remember that in a plasma like the corona and the solar wind, the abundance of oxygen and other heavy ions is very small. They are basically test particles. Ion cyclotron waves at the gyrofrequency of these minor ions and its neighborhood can comfortably exist while heating these ions substantially. This also means that when a broad spectrum of ion cyclotron waves exist, all particles in oxygen velocity space can be accelerated simultaneously in the direction perpendicular to the background magnetic field. As a result, the void at the center is possible when all oxygen ions are simultaneously accelerated by ion cyclotron waves. For the major species protons, this is impossible since the frequency of ion cyclotron waves is always smaller than the proton gyrofrequency and only protons with negative velocity can resonate with these waves. Hence we can predict that protons in the solar wind which resonate with ion cyclotron waves can never have velocity distributions as those shown in Figure 6. We will see that this is indeed the case in the next section.

[17] Figures 5 and 6 also demonstrate that the velocity distribution of minor ions under the influence of ion cyclotron waves evolves dramatically with time. This fact has implications for the treatment of ion heating using quasi-linear theory of ion cyclotron resonance. Quasi-linear theory assumes that the deviation from averaged velocity distribution is small under the influence of ion cyclotron resonance. However, this may not be true for minor ions. Hence our results suggest that the quasi-linear theory cannot be applied to minor ions.

[18] It is noted that ring velocity distributions of oxygen were also found in a study by *Lee and Wu* [2000], who used

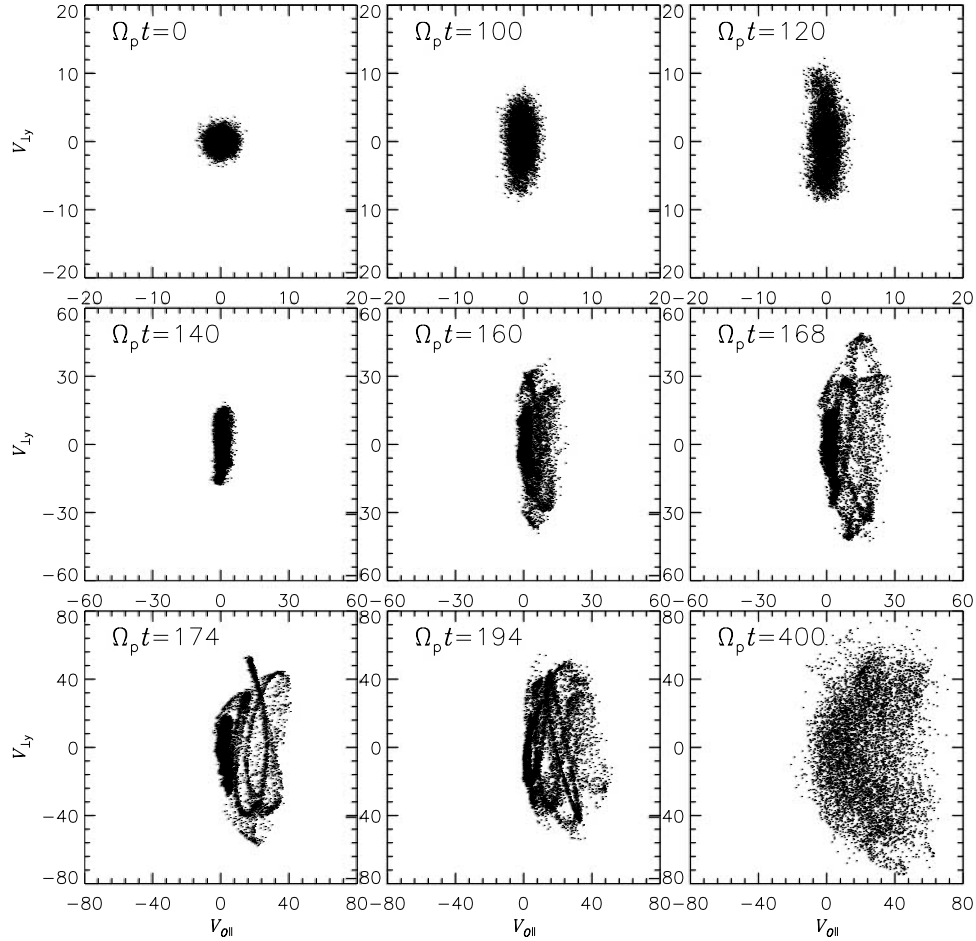


**Figure 5.** Scatterplots of oxygen  $O^{+5}$  velocity in the plane parallel to the background magnetic field. Velocities are in units of the oxygen thermal speed  $U_O$  at  $\Omega_p t = 0$ . Note that the velocity scale in subsequent rows changes.

a fast shock heating mechanism for the fast solar wind. In their studies, they found that fast shocks are able to achieve an oxygen temperature anisotropy as large as  $T_{O\perp}/T_{O\parallel} \approx 50$  and a proton temperature anisotropy of  $T_{p\perp}/T_{p\parallel} \approx 1.2$ . These shocks are also able to accelerate the fast solar wind to observed velocities.

### 3.2. Heating of Protons

[19] In this section, we present the property of protons under the influence of ion cyclotron waves. Figure 7 shows the temporal evolution of proton temperatures, anisotropy and bulk flow speed. The heating of protons lags oxygen heating (see Figure 4). This is understandable since the growth rates of the high frequency waves which are able to resonate with protons are smaller than the growth rates of those low frequency waves which can readily resonate with oxygen ions (see Figure 1). Hence it takes a longer time for those high frequency waves to grow stronger enough to influence protons. The magnitude of proton heating is significantly smaller than that of oxygen ions. After  $\Omega_p t \geq 250$  the temperature of oxygen ions is more than 100 times higher than that of protons. The combination of the small oxygen abundance and more wave power at low frequencies enables oxygen ions to be heated more dramatically than protons.

[20] Figure 7a shows very little parallel heating of the protons. This is very different from the heating of oxygen ions shown in Figure 4. This suggests that in a low beta plasma, protons can maintain a significant temperature anisotropy.

[21] As protons are mainly heated in the perpendicular direction, there is a bulk acceleration as well. Again, the magnitude of this acceleration is significantly smaller than that of oxygen ions. As a result, oxygen ions can flow much faster than protons. At  $\Omega_p t = 400$  the differential flow speed between oxygen ions and protons is  $0.36v_A$ . Compared with Figure 4c, the perpendicular fluid velocity of protons (dotted line in Figure 7c) is much smaller than that of oxygen ions.

[22] Figures 8 and 9 show the scatterplots of proton velocity in the plane parallel and perpendicular to the background magnetic field at the same times as shown in Figures 5 and 6. Obviously, proton velocity distributions under the influence of ion cyclotron waves are far less complex than those of oxygen ions. All scatterplots in Figure 8 show that proton velocity distributions are roughly bi-Maxwellian or Maxwellian. Since only protons with negative velocity can resonate with ion cyclotron waves, the near bi-Maxwellian proton velocity distributions suggest that some very fast physical processes may be at work.

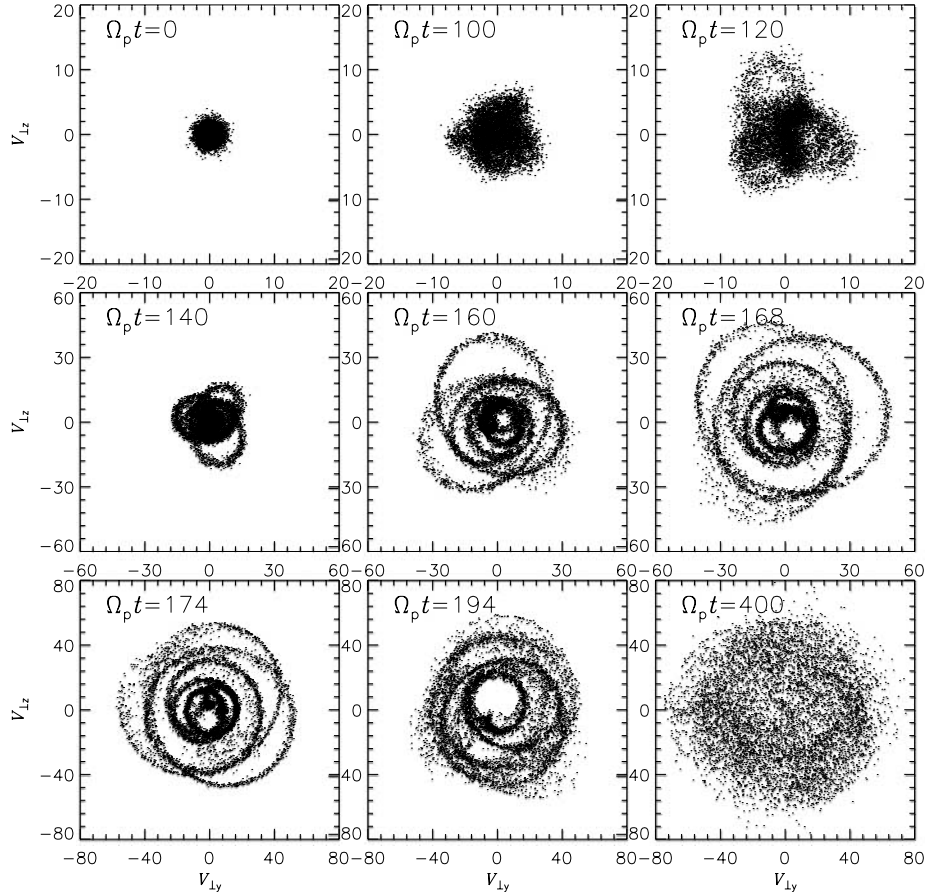


**Figure 6.** Scatterplots of oxygen  $O^{+5}$  velocity in the velocity plane perpendicular to  $v_{\parallel}$ . Velocities are in units of the oxygen thermal speed  $U_O$  at  $\Omega_p t = 0$ . Note that the velocity scale in subsequent rows changes.

[23] Figure 9 demonstrates that in the plane perpendicular to the background magnetic field, proton velocity distributions remain gyrotropic. No ring-like distribution exists. Again, this is because ion cyclotron waves can only exist below the proton gyrofrequency. It is impossible for all protons in the phase space to be simultaneously accelerated in the perpendicular direction.

### 3.3. Wave Amplitude and the Abundance of Oxygen Ions

[24] We conclude this section by briefly discussing some relevant issues. In the case presented above, the abundance of oxygen ions is fixed at  $10^{-5}$ . *Ofman et al.* [2001, 2002] have used a relatively large abundance. We found that if we increase the abundance to  $10^{-4}$ , protons do not undergo a noticeable change. The overall results for oxygen ions remain the same as well. This suggests that as long as minor ions are test particles, our results will hold.

[25] Although the amplitude of ion cyclotron waves in the near Sun solar wind is unknown, the wave amplitude produced by  $Li^{+1}$  ions in the case presented above is perhaps relatively too large for conditions in the solar wind at several solar radii. We have run some test cases with the abundance of  $Li^{+1}$  smaller than 0.075. In those cases, the maximum growth rate of ion cyclotron waves due to the temperature anisotropy instability of  $Li^{+1}$  is significantly smaller than that in Figure 1. Hence it takes a longer time for the instability to be fully developed and the simulations

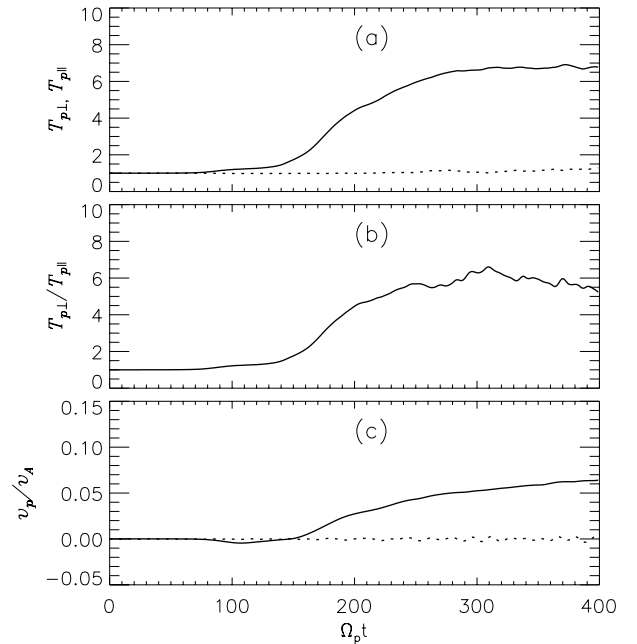


**Figure 7.** Evolution of (a) proton parallel (dotted line) and perpendicular (solid line) temperature, (b) temperature anisotropy  $T_{p\perp}/T_{p\parallel}$ , and (c) flow speed along background magnetic field (solid line) and perpendicular fluid speed  $v_y$  (dotted line). The temperatures are in units of initial temperature.

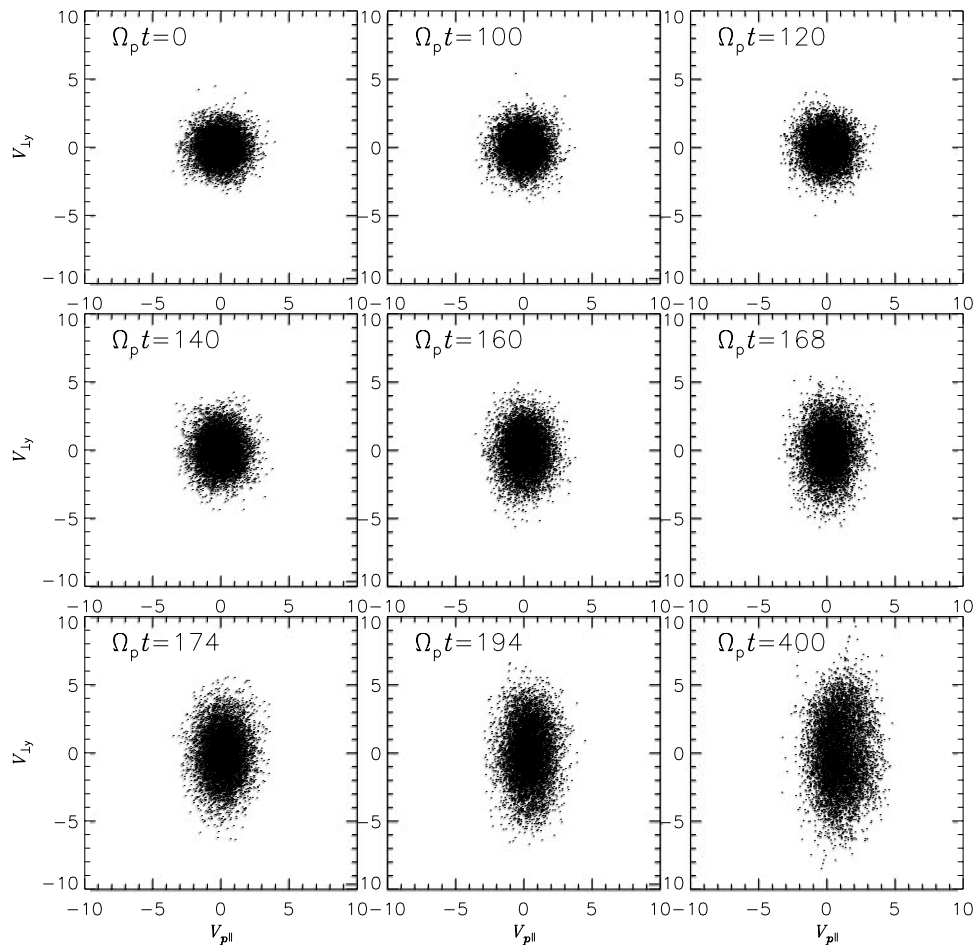


**Figure 8.** Scatterplots of proton velocity in the plane parallel to the background magnetic field. Velocities are in units of proton thermal speed  $U_p$  at  $\Omega_p t = 0$ .

take more computing time. However, the physics presented above remains the same: the same figures as presented in Figures 4–9 for these cases will look very similar. However, the magnitude of heating and acceleration will be less pronounced. For example, if  $n_{Li}/n_p = 0.03$ , and other parameters do not change, it is found that at  $\Omega_p t = 600$ , the bulk flow speed of oxygen ions will be about  $0.24v_A$  and oxygen perpendicular and parallel temperature will be about 500 and 100 times of their initial temperature.

#### 4. Concluding Remarks

[26] We investigated the property of oxygen ions and protons under the influence of a broadband spectrum of ion cyclotron waves generated by plasma micro-instabilities. It is shown that oxygen ions and protons can develop a strong temperature anisotropy with preferential heating in the perpendicular direction in an initially low beta plasma such as in the extended solar corona. Oxygen ions are preferentially heated and accelerated. Owing to ion cyclotron waves, oxygen heating and acceleration may have two stages. During the first stage, oxygen ions are accelerated and heated in the direction perpendicular to the background magnetic field and can develop an extremely high temperature anisotropy with  $T_{O\perp}/T_{O\parallel} \approx 22$  in an initially low beta

plasma (beta value at 0.01). However, very little parallel heating is observed. Hence, during this stage, oxygen ions do not show appreciable bulk acceleration along the background magnetic field. In the second stage, a large bulk acceleration of oxygen ions (as large as 0.3 Alfvén speed) is observed. As a result, ion cyclotron waves are not able to maintain the high temperature anisotropy as resonant heating continues. In the second stage, because of the small abundance of oxygen ions, the nonlinear nature of wave particle interaction yields to highly complex velocity distributions. The existence of ion cyclotron waves at the oxygen gyrofrequency also generates significant perpendicular fluid velocity fluctuations but the magnitude is still much smaller than the perpendicular thermal speed of resonantly heated oxygen ions. Since both perpendicular fluid velocity fluctuations and thermal motions broaden spectral lines observed by UVCS/SOHO, this suggests that the perpendicular fluid velocity fluctuations are less important than thermal motions in broadening spectral lines of minor ions if ion cyclotron waves are indeed responsible for the heating of these ions. In our studies, proton velocity distributions remain near bi-Maxwellian. *Ofman et al.* [2002] have shown that when protons are heated by cyclotron waves with smaller wave amplitudes, proton velocity distributions also remain near bi-Maxwellian. Our

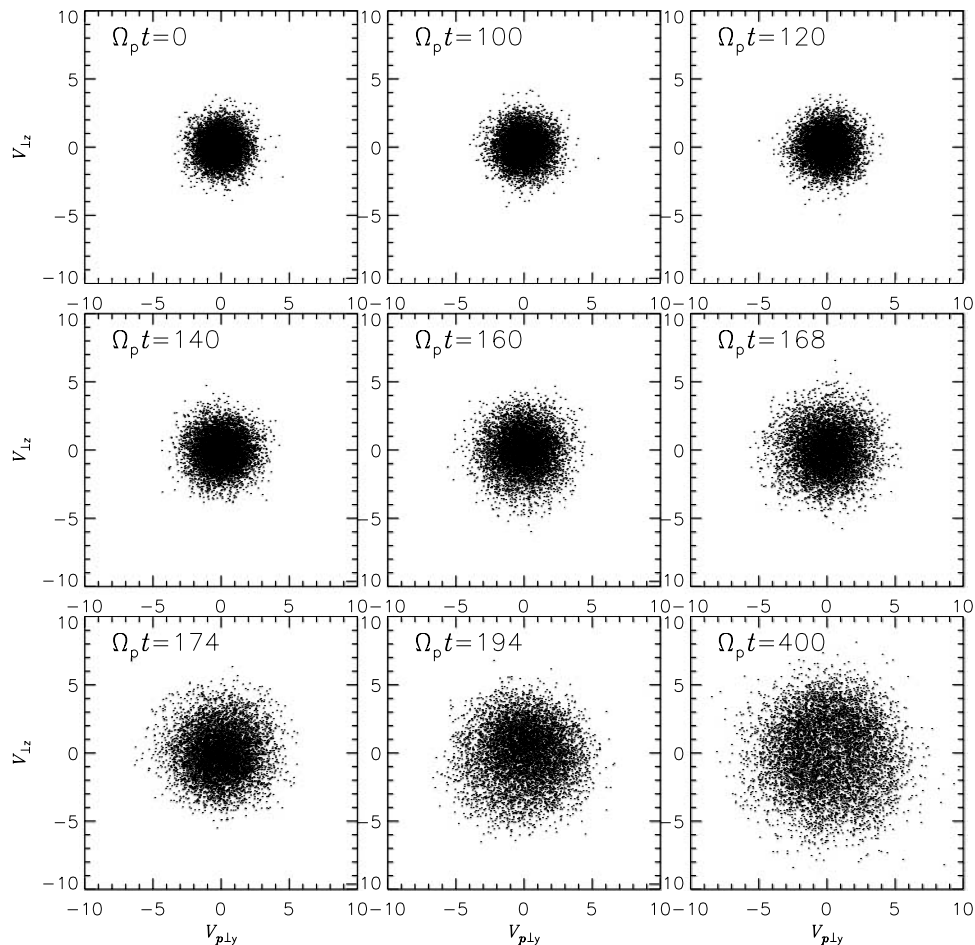


**Figure 9.** Scatterplots of proton velocity in the velocity plane perpendicular to  $v_{\parallel}$ . Velocities are in units of proton thermal speed  $U_p$  at  $\Omega_p t = 0$ .

results suggest that quasi-linear theory may be not valid for the treatment of minor ions.

[27] The simulation described here shows that perpendicular heating of oxygen ions and protons by ion cyclotron waves is much stronger than it was found by other authors in similar studies [Liewer *et al.*, 2001; Ofman *et al.*, 2002; Gary and Saito, 2003]. One possible reason is that the amplitude of ion cyclotron waves in this study is much larger than the amplitude of externally driven ion cyclotron waves used in those studies. Currently we do not have empirical knowledge of the properties (e.g., amplitude, spectral distribution) of these waves at several solar radii in the fast solar wind which is of interest to this paper. In hybrid models, it is difficult to introduce large amplitude externally driven highly nonlinear ion cyclotron waves in a completely self-consistent manner. If this can be done, a future work adopting large amplitude externally driven ion cyclotron waves is appropriate to explore the acceleration effect further.

[28] This study has implications for the observation of oxygen temperature anisotropy in the inner corona. The first study [Li *et al.*, 1998] of temperature anisotropy on the observation of oxygen ions showed that the intensity ratio between OVI 1032 and OVI 1037 lines is not sensitive to the temperature anisotropy of  $O^{+5}$  ions when the pumping by carbon lines is properly accounted for and if we assume

the broad line profiles of oxygen lines observed by Kohl *et al.* [1997] to be due mainly to a high kinetic temperature. This study showed that ion cyclotron waves, which are widely thought to be responsible for the large temperature anisotropy of 10–100 reported by Cranmer *et al.* [1999], cannot maintain such a large anisotropy in the inner corona. Tu and Marsch [2001] also reached the same conclusion with a fluid approach and question the role of these waves. One has to know that the high temperature anisotropy reported by Cranmer *et al.* [1999] was derived from observations and not directly observed [see Li *et al.*, 1999]. Many parameters such as electron density, the geometry of magnetic field, the detailed oxygen velocity distributions and the intensity of spectral lines such as the oxygen and carbon doublets can all influence the determination of the temperature anisotropy.

[29] **Acknowledgments.** This work is supported by a PPARC rolling grant to University of Wales, Aberystwyth. Part of the work is also supported by a NASA grant to the Smithsonian Astrophysical Observatory.

[30] Lou-Chuang Lee thanks S. Peter Gary and B. H. Wu for their assistance in evaluating this paper.

## References

Arunasalam, V. (1976), Quasilinear theory of ion-cyclotron-resonance heating of plasmas and associated longitudinal cooling, *Phys. Rev. Lett.*, 37, 746.

- Cranmer, S. R. (2000), Ion cyclotron wave dissipation in the solar corona: The summed effect of more than 2000 ion species, *Astrophys. J.*, *532*, 1197.
- Cranmer, S. R., G. B. Field, and J. L. Kohl (1999), Spectroscopic constraints on models of ion cyclotron resonance heating in the polar solar corona and high-speed solar wind, *Astrophys. J.*, *518*, 937.
- Dusenbery, P. B., and J. V. Hollweg (1981), Ion-cyclotron heating and acceleration of solar wind minor ions, *J. Geophys. Res.*, *86*, 152.
- Galinsky, V. L., and V. I. Shevchenko (2000), Nonlinear cyclotron resonant wave particle interaction in a non-uniform magnetic field, *Phys. Rev. Lett.*, *85*, 90.
- Gary, S. P., and S. Saito (2003), Particle-in-cell simulations of Alfvén-cyclotron wave scattering: Proton velocity distributions, *J. Geophys. Res.*, *108*(A5), 1194, doi:10.1029/2002JA009824.
- Gary, S. P., L. Yin, D. Winske, and L. Ofman (2001), Electromagnetic heavy ion cyclotron instability: Anisotropy constraint in the solar corona, *J. Geophys. Res.*, *106*, 10,715.
- Gary, S. P., et al. (2003), Consequences of proton and alpha anisotropies in the solar wind: Hybrid simulations, *J. Geophys. Res.*, *108*(A2), 1068, doi:10.1029/2002JA009654.
- Hollweg, J. V. (1999), Cyclotron resonance in coronal holes, 2. A two-proton description, *J. Geophys. Res.*, *104*, 24,793.
- Hollweg, J. V. (2000), Cyclotron resonance in coronal holes, 3. A five-beam turbulence driven model, *J. Geophys. Res.*, *105*, 15,699.
- Hollweg, J. V., and P. A. Isenberg (2002), Generation of the fast solar wind: A review with emphasis on the resonant cyclotron interaction, *J. Geophys. Res.*, *107*(A7), 1147, doi:10.1029/2001JA000270.
- Hu, Y. Q., and S. R. Habbal (1999), Resonant acceleration and heating of solar wind ions by dispersive ion cyclotron waves, *J. Geophys. Res.*, *104*, 17,045.
- Isenberg, P. A. (2004), The kinetic shell model of coronal heating and acceleration by ion cyclotron waves: 3. The proton halo and dispersive waves, *J. Geophys. Res.*, *109*, A03101, doi:10.1029/2002JA009449.
- Isenberg, P. A., M. A. Lee, and J. V. Hollweg (2001), The kinetic shell model of coronal heating and acceleration by ion cyclotron waves: 1. Outward propagating waves, *J. Geophys. Res.*, *106*, 5649.
- Kohl, J. L. (1998), UVCS/SOHO empirical determinations of anisotropic velocity distributions in the solar corona, *Astrophys. J.*, *501*, 127L.
- Kohl, J. L., et al. (1997), First results from the SOHO ultraviolet coronagraph spectrometer, *Solar Phys.*, *175*, 613.
- Lee, L. C., and B. H. Wu (2000), Heating and acceleration of protons and minor ions by fast shocks in the solar corona, *Astrophys. J.*, *535*, 1014.
- Li, X. (2003), Transition region, coronal heating and the fast solar wind, *Astron. Astrophys.*, *406*, 345.
- Li, X., and S. R. Habbal (1999), Ion cyclotron waves, instabilities and solar wind heating, *Sol. Phys.*, *190*, 485.
- Li, X., S. R. Habbal, J. L. Kohl, and G. C. Noci (1998), The effect of temperature anisotropy on observations of Doppler dimming and pumping in the inner corona, *Astrophys. J.*, *501*, L133.
- Li, X., S. R. Habbal, J. V. Hollweg, and R. Esser (1999), Heating and cooling of protons by turbulence-driven ion cyclotron waves in the fast solar wind, *J. Geophys. Res.*, *104*, 2521.
- Liewer, P. C., M. Velli, and B. E. Goldstein (2001), Alfvén wave propagation and ion cyclotron interactions in the expanding solar wind: One-dimensional hybrid simulations, *J. Geophys. Res.*, *106*, 29,261.
- Lu, Q. M., and S. Wang (2005), Proton and He<sup>2+</sup> temperature anisotropies in the solar wind driven by ion cyclotron waves, *Chin. J. Astron. Astrophys.*, *5*, 184.
- Marsch, E., C. K. Goertz, and K. Richter (1982), Wave heating and acceleration of solar wind ions by cyclotron resonance, *J. Geophys. Res.*, *87*, 5030.
- Ofman, L., A. Vinas, and S. P. Gary (2001), Constraints on the O<sup>+</sup> anisotropy in the solar corona, *Astrophys. J.*, *547*, L175.
- Ofman, L., S. P. Gary, and A. Vinas (2002), Resonant heating and acceleration of ions in coronal holes driven by cyclotron resonant spectra, *J. Geophys. Res.*, *107*(A12), 1461, doi:10.1029/2002JA009432.
- Stix, T. H. (1992), *Waves in Plasmas*, Springer, New York.
- Tam, S. W. Y., and T. Chang (2001), Effect of electron resonant heating on the kinetic evolution and acceleration of the solar wind, *Geophys. Res. Lett.*, *28*, 1351.
- Tu, C.-Y., and E. Marsch (2001), On cyclotron wave heating and acceleration of solar wind ions in the outer corona, *J. Geophys. Res.*, *106*, 8233.
- Tu, C.-Y., E. Marsch, K. Wilhelm, and W. Curdt (1998), Ion temperatures in a solar polar coronal hole observed by SUMER on SOHO, *Astrophys. J.*, *503*, 475.
- Vocks, C. (2002), A kinetic model for ions in the solar corona including wave-particle interactions and Coulomb collisions, *Astrophys. J.*, *568*, 1017.
- Vocks, C., and E. Marsch (2001), A semi-kinetic model of wave-ion interactions in the solar corona, *Geophys. Res. Lett.*, *28*, 1917.
- Vocks, C., and E. Marsch (2002), Kinetic results for ions in the solar corona with wave-particle interactions and Coulomb collisions, *Astrophys. J.*, *568*, 1030.
- Winske, D., and N. Omidi (1993), Hybrid codes: Methods and applications, in *Computer Space Plasma Physics: Simulation Techniques and Software*, edited by H. Matsumoto and Y. Omura, p. 103, Terra Sci., Tokyo.
- Xie, H., L. Ofman, and A. Vinas (2004), Multiple ions resonant heating and acceleration by Alfvén/cyclotron fluctuations in the corona and the solar wind, *J. Geophys. Res.*, *109*, A08103, doi:10.1029/2004JA010501.

S. R. Habbal, Institute for Astronomy, University of Hawaii, 2680 Woodlawn Drive, Honolulu, HI 96822, USA.

X. Li, Institute of Mathematical and Physical Sciences, University of Wales, Aberystwyth, SY23 3BZ UK. (xxl@aber.ac.uk)